Hindawi Publishing Corporation
Advances in Electrical Engineering
Volume 2016, Article ID 8039679, 17 pages
http://dx.doi.org/10.1155/2016/8039679

Research Article

Comparison of 6 Diode and 6 Transistor Mixers Based on Analysis and Measurement

J. Ladvánszky[1] and K. M. Osbáth[2]

[1]*Ericsson Telecom Hungary Ltd., Irinyi József Utca 4-20, Budapest 1117, Hungary*
[2]*Department of Broadband Infocommunications and Electromagnetic Theory, Budapest University of Technology and Economics, Egry József Utca 18, Budapest 1111, Hungary*

Correspondence should be addressed to J. Ladvánszky; janos.ladvanszky@ericsson.com

Received 7 March 2016; Accepted 6 April 2016

Academic Editor: Mamun B. Ibne Reaz

Our goal is to overview semiconductor mixers designed for good large signal performance. Twelve different mixers were compared utilizing pn diodes, bipolar transistors, and/or junction field effect transistors. The main aspect of comparison is the third-order intercept point (IP3), and both circuit analysis and measurement results have been considered. IP3 has been analyzed by the program AWR (NI AWR Design Environment) and measured by two-tone test (Keysight Technologies). We provide three ways of improvement of large signal performance: application of a diplexer at the RF port, reduction of DC currents, and exploiting a region of RF input power with infinite IP3. In addition to that, our contributions are several modifications of existing mixers and a new mixer circuit (as illustrated in the figures). It is widely believed that the slope of the third-order intermodulation product versus input power is always greater than that of the first-order product. However, measurement and analysis revealed (as illustrated in the figures) that the two lines may be parallel over a broad range of input power, thus resulting in infinite IP3. Mixer knowledge may be useful for a wide range of readers because almost every radio contains at least one mixer.

1. Introduction

During the last decade, mixer research reached a quiescent point. It is time to look back and make an overview. This is the main goal of our paper. A mixer is a three-port device having two inputs (RF and LO, radio frequency and local oscillator, resp.) and one output (IF, intermediate frequency). It is used, for example, to convert the RF signal (that may be of variable frequency) to a fixed IF, because filtration is easier at a fixed frequency. In this paper we use fixed RF. At the RF and LO ports, periodic excitations are applied, with fundamental angular frequencies $\omega_1, \omega_2, \ldots$ and ω_{LO}, respectively, and we are interested in the IF signals at $\omega_1 \pm \omega_{\mathrm{LO}}, \omega_2 \pm \omega_{\mathrm{LO}}, \ldots$. These are the useful IF signals or first-order products. Higher order intermodulation products are also present at the IF port, and among them the third-order products are the most disturbing ones because if $\omega_1 \pm \omega_{\mathrm{LO}}$ and $\omega_2 \pm \omega_{\mathrm{LO}}$ are near to each other, then the third-order intermodulation products at $2\omega_1 - \omega_2 \pm \omega_{\mathrm{LO}}$ and $2\omega_2 - \omega_1 \pm \omega_{\mathrm{LO}}$ are also near to the useful signals.

The mixing effect (time domain multiplication of the RF signal by the LO signal) is a result of nonlinearity and/or time variance. It can be modeled by time-invariant nonlinear and/or time-varying linear circuit elements, depending on whether the LO signal is a sinusoid or a square. Both can be treated by Fourier analysis [1]. The big difference between them is that a time-invariant nonlinear circuit element always produces intermodulation, while a time-varying linear circuit element never does it. For this reason, to reach low intermodulation, it is advantageous to apply square LO signal or sinusoid of high amplitude. The reason is that, for a square LO signal, semiconductor will contribute (almost) as time-varying element and does not produce intermodulation, and a similar thing occurs in case of large sinusoidal LO. The simplest time-varying linear circuit element is an ideal switch. The practical situation usually is that both nonlinear

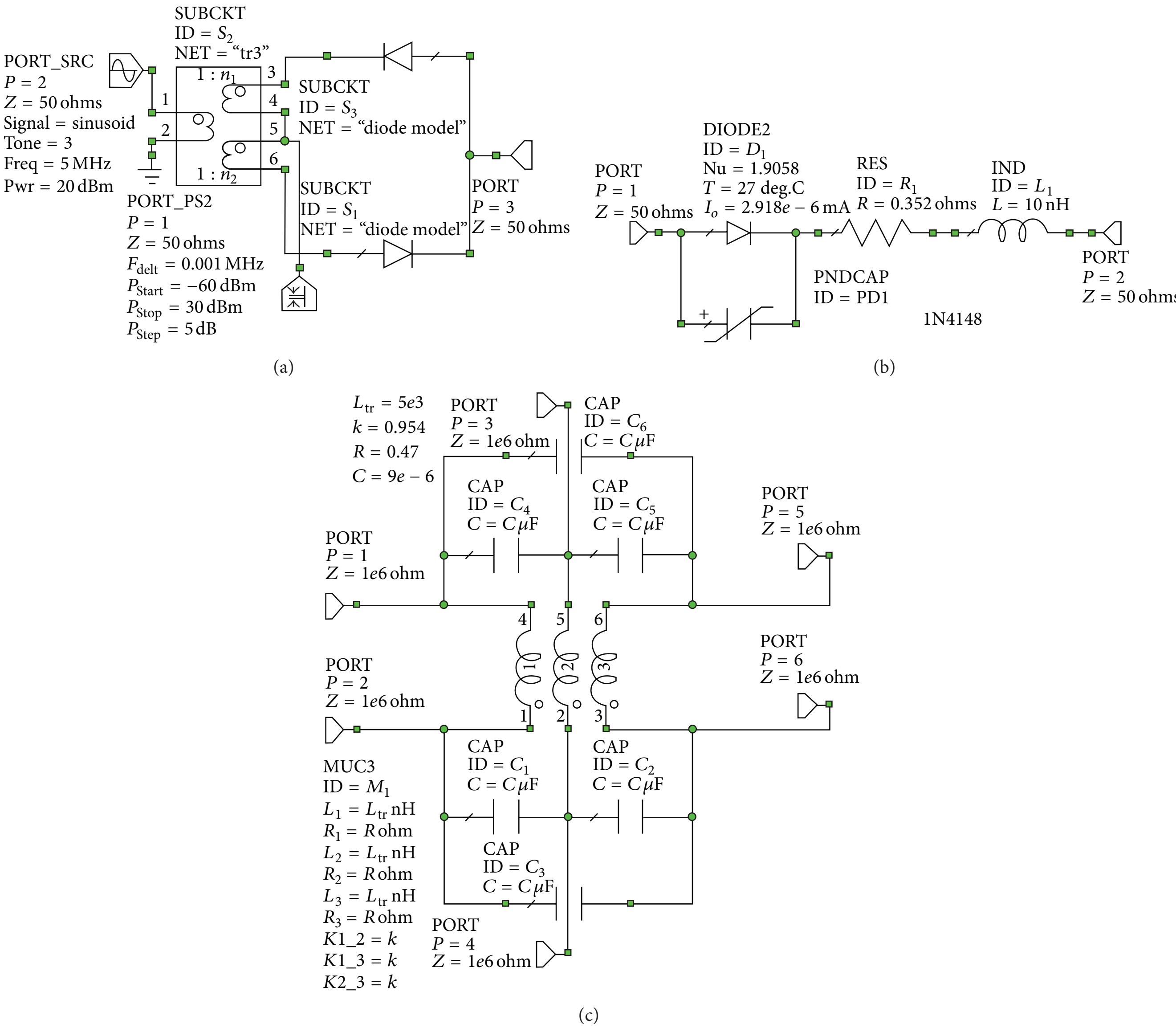

Figure 1: (a) Schematics of the two-diode mixer. (b) Diode model for Figures 1(a), 2, 3, 4, and 5. (c) Model of the three-coil transformer tr3 for Figures 1(a), 2, 3(a), 4, 5, 6, 7(a), 8, 9, 10, and 11. Model parameters were optimized with the goals of inductance of one coil, when the others are both terminated by open circuit or one is shorted, and capacitance between ends of coils at the same side, all measured at 5 MHz.

and time-varying effects are present and are difficult to distinguish.

Third-order intercept point IP3 is a power level where the straight lines fit to the first- and third-order IF output power versus RF input power curves intersect each other. With the condition that the slope of the third-order IF product versus RF input power is three times as much as that of the first-order product, the higher the IP3 is, the smaller the disturbance caused by the third-order intermodulation is. IIP3 and OIP3 are the input and output third-order intercept points, respectively. Their difference is the conversion loss.

Another important mixer characteristic is the 1 dB compression point $P_{1\,\mathrm{dB}}$. It is the RF input power when the first-order IF versus RF curve saturates by 1 dB.

In this paper, we compare twelve different mixer configurations: a two-diode mixer [2], a diode ring mixer [3], a triple balanced mixer with diodes [4], a rectifier-like mixer [5], a half H mixer with diodes (our contribution), a full H mixer with diodes [6], a four-quadrant multiplier [7] modified by us, a half H mixer [8], Russian version [6] of the half H mixer modified by us, the original full H mixer [6], a full H mixer simplified by us, and an FET ring mixer [9]. We excluded from the comparison the transmission line transformer version of the triple balanced mixer [10] because, in the analysis, it did not behave like triple balanced. Main aspect of comparison is IP3, but we include conversion loss and LO to RF and LO to IF isolations as well.

In Section 2, the qualitative theory of operation using switches is obtained. In Section 3, large signal analysis results are compared. For large signal analysis, we use the harmonic balance method [12]. Measurements are included in Section 4. We apply here the two-tone test [13]. In Section 5,

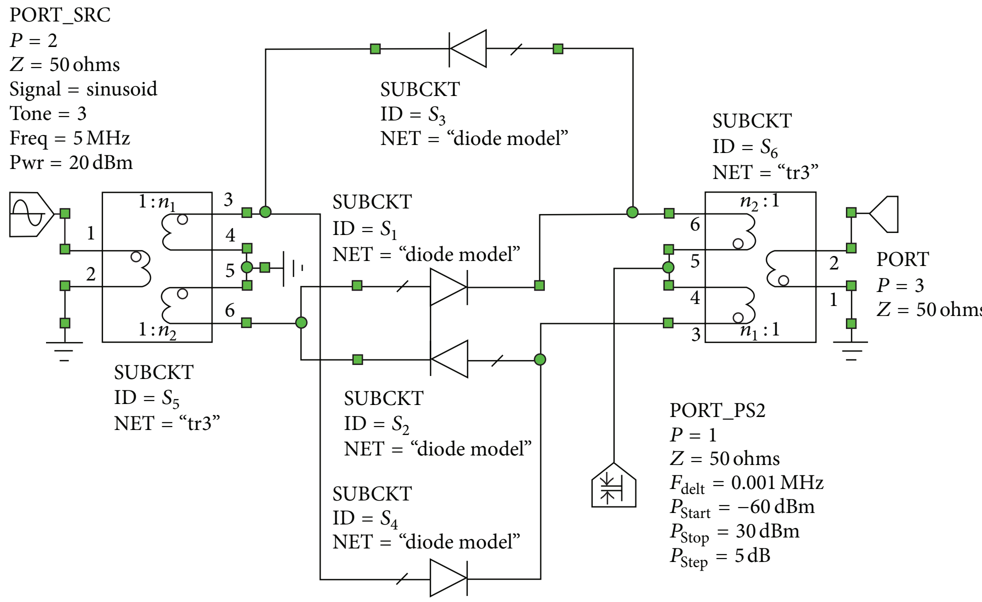

Figure 2: Schematics of the diode ring mixer.

three ways for improvement of large signal performance have been obtained; however, this knowledge has not been published yet: application of a diplexer at RF port, reduction of DC currents, and exploiting an RF range with infinite IP3 [14].

Recently, many fine papers about mixers have appeared (e.g., [15, 16]). The difference between those papers and this one is that our intention is to provide an overview based on agreement of analysis and measurement results. Therefore, all mixers are analyzed, built up, and measured under the same conditions; see please Sections 3 and 4.

This is a preparatory work to design microwave mixers. Our concept is to check large signal performance first at a few MHz, as it has been done here, and then to turn to microwave mixer design, in a later publication. With this step, investigations of large signal performance and frequency dependence have been somewhat separated.

For understanding the schematics, basic knowledge of the analysis program AWR [17] is necessary.

This paper introduces a unified terminology in mixer names, has tutorial value by overviewing such mixers that are rarely used or not so widely known, and includes novelties such as our modifications to well-known mixer topologies and a new mixer circuit, which contains a proof by analysis and measurement in agreement that IP3 can be infinite, and a method how to generate an RF input power region with infinite IP3 [14].

2. Qualitative Theory of Operation

In this section we idealize circuit operation by replacing semiconductors by switches whenever possible. From this point of view, operation of all mixers is based on the fact that RF signal appears at the IF port with polarity changed in the pace of the LO signal. The first mixer is an exception as we observe. Note that, for the qualitative theory of operation, RF signal is always assumed to be negligible as compared to the LO signal. Numbering of ports is the same for all mixers: Ports 1, 2, and 3 are the RF, LO, and IF ports, respectively.

Schematics of the first mixer are shown in Figure 1.

All schematics are imported from AWR. RF input is two-tone excitation at 4 MHz, frequency difference is 1 kHz, LO signal is at 5 MHz, and we look for intermodulation products around 9 MHz at the IF port (here arbitrary frequencies can be chosen in the few MHz range). Here RF power is swept from −60 to 30 dBm by 5 dBm. If the RF signal is small, then, for the positive and negative half periods of the LO signal, both diodes are opened or shorted, respectively. For the positive half period, IF port is not connected. For the negative half period, RF port is connected to the IF port through the transformer. Since only half of the LO period is exploited, therefore conversion loss is high.

For the diode ring mixer (Figure 2), if the RF signal is small, then, for the positive half period of the LO signal, the lower two diodes are open, and, for the negative half period, the upper two. Therefore, the RF signal appears at the lower left or the upper left winding of the IF transformer, respectively. As these windings are connected oppositely to each other, polarity of the RF signal is changed at the right winding in pace of the LO signal.

If we compare Figures 1 and 2, we can realize that the diode ring mixer can be built using two 2-diode mixers, while carefully adding their IF output signals. On the contrary, with the 2-diode mixer, both half periods of the LO are exploited; thus the conversion loss is much less than that of the 2-diode mixer.

In Figure 3, during the positive half period of the LO, S_2 and S_3 of the upper quad and S_6 and S_7 of the lower quad conduct, the RF signal is connected through transformers to the IF transformer. In the other half period of the LO,

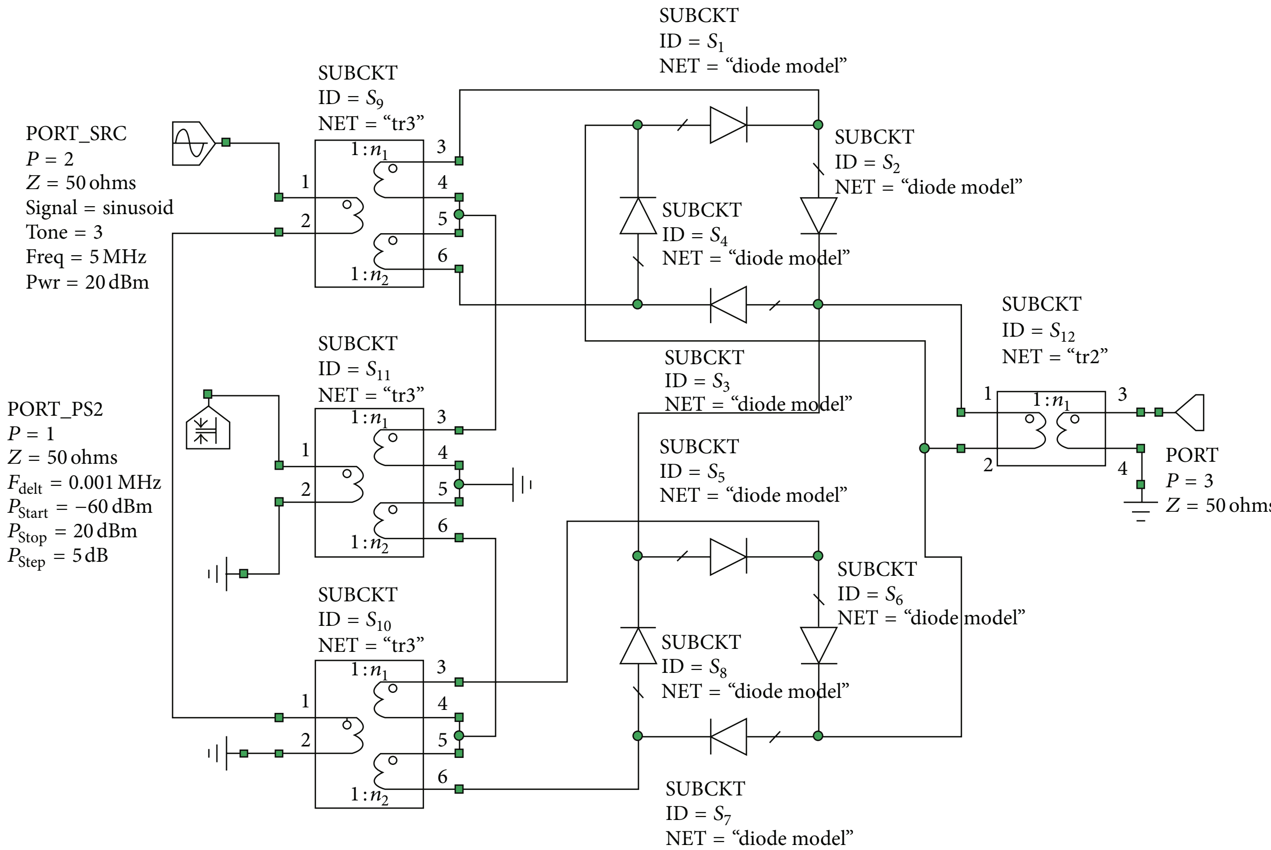

(a)

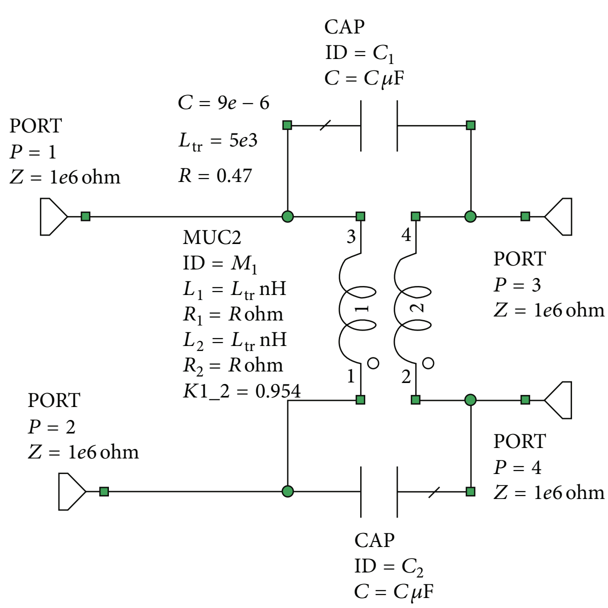

(b)

Figure 3: (a) Schematics of the triple balanced mixer with diodes. (b) Model of the two-coil transformer tr2 for Figures 3(a), 4, and 8.

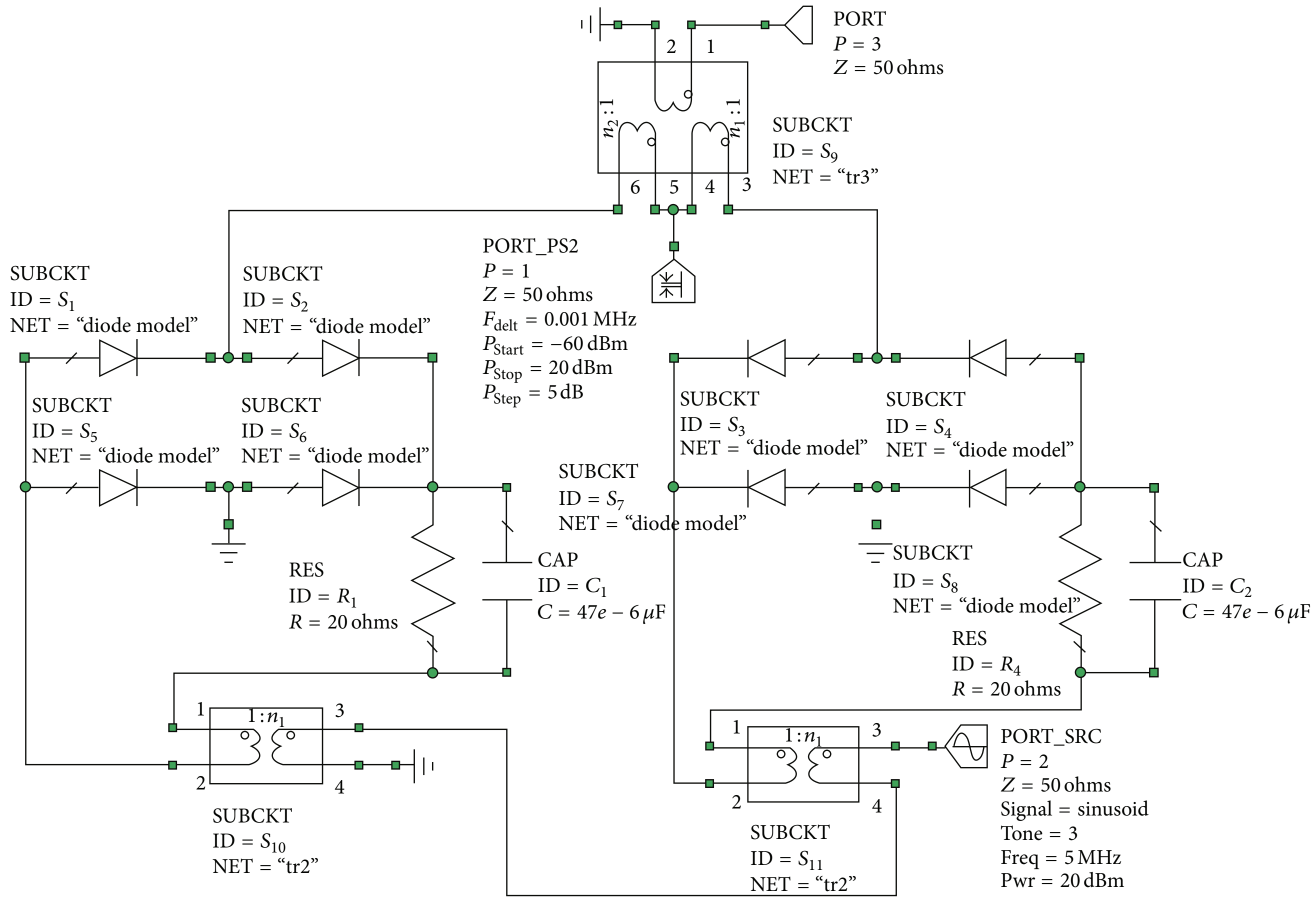

Figure 4: Schematics of the rectifier type mixer with diodes. Differences with respect to the original one [5] are separation of LO transformers and inclusion of capacitors; these are our contributions to increase IP3.

the remaining diodes will conduct and reverse the polarity of RF at the IF transformer.

Figures 1, 2, and 3 diodes were connected in the way that a cathode was connected to an anode. The mixer in Figure 4 is basically different. Interconnection of diodes in quads is similar to a rectifier; for this reason it is known as the rectifier type mixer. For the positive half period of the LO, all four diodes on the right are switched on and the other four are switched off. Through diodes that are switched on, the lower right winding of the IF transformer is grounded; thus a current from the RF input flows, inducing a voltage in the winding at the top that is connected to the IF output. In the other half period, current flows in the winding at the lower left, which is connected to opposite direction as compared to the middle winding. So at the IF port, RF signal will be present with opposite polarity in every half period of the LO.

Role of the resistors is to limit the DC currents while the capacitors provide high AC currents. Role of separation of LO transformers is that the diode quads cannot interact through magnetic field, but only through voltages and currents.

Figure 5 shows our contribution, the so-called half H mixer with diodes. The name half H comes from the uppercase letter H. Half of the letter below the horizontal symmetry axis is deleted, and, in the vertical branches, three-coil transformers of the full H in Figure 6 are replaced by two-coil ones.

The diodes are switched on alternatively. Thus, in the secondary of the transformer at the middle, either the left or the right part couples the RF signal to the IF port, with opposite polarities.

In Figure 6, in the pace of the LO signal, either S_1 and S_4 or S_2 and S_3 diodes are open. Thus, direction of the RF signal is altered at the IF port in the pace of the LO signal.

In Figures 7(a) and 7(b), the well-known four-quadrant multiplier is shown. LO switches and amplifiers were realized by jFETs and BJTs, respectively. As linearity of both stages is high, very good large signal properties are achieved, as shown in Table 1.

In Figure 8(a), at the positive LO half period, upper right winding of the transformer on the right is grounded, while, in the other half period, winding at the lower right is grounded. Thus, the voltage induced in the winding on the left of S_4 is proportional to the RF voltage, changing polarity at the pace of the LO signal.

In Figure 9, in the positive half period of the LO, S_1 is conductive and S_2 is open. This means that RF signal reaches

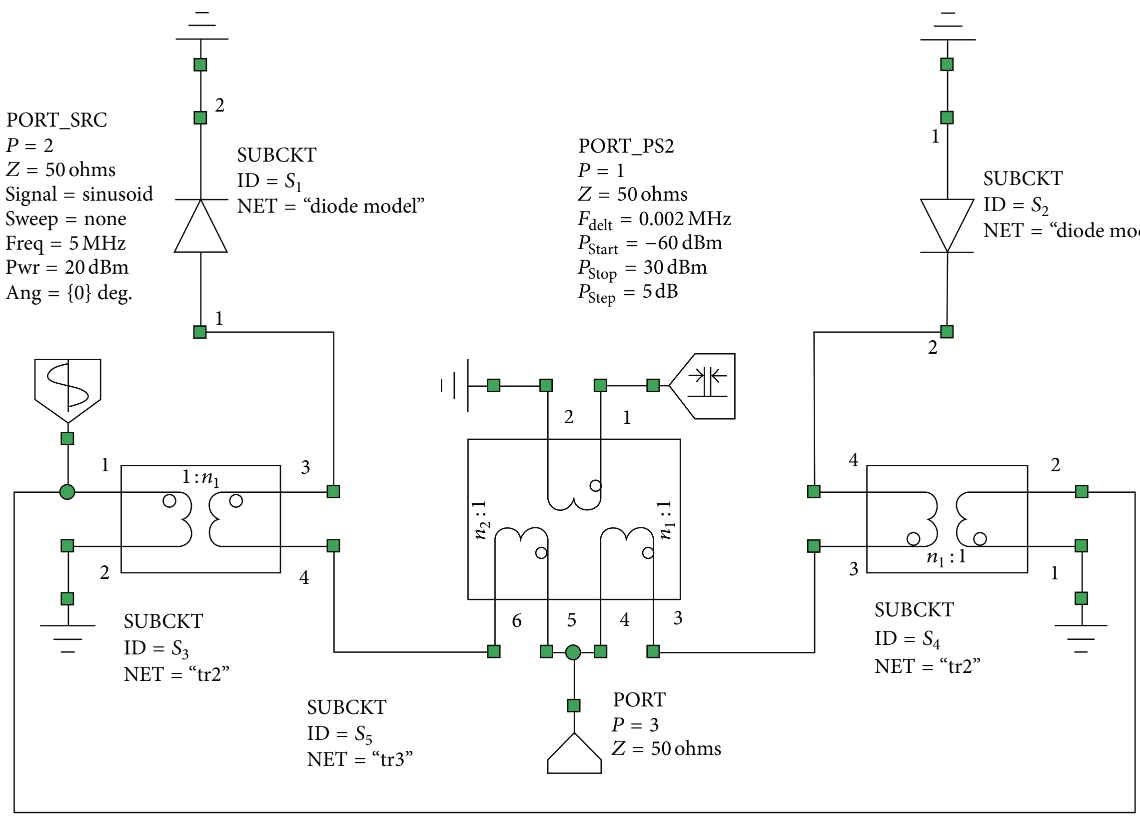

Figure 5: Schematics of the half H mixer with diodes.

the IF port through S_4, while the secondary of S_5 is grounded. In the other half period of the LO, RF signal reaches the IF port through S_5, while the secondary of S_4 is grounded. As a result, RF signal changes polarity at the IF port in the pace of the LO signal.

Motivation of the mixer in Figure 10 was to change the direction of RF signal at IF port with pace of LO in such a way that GS voltages of the switches should not be modulated by RF. For the positive LO half period, upper left and lower right switches are on, and, during the other half period, upper right and lower left are on. Thus, the RF voltage is transferred to the upper winding of the IF transformer with opposite polarity in every LO half period.

In Figure 11, for the positive LO half period, upper left and lower right switches are on, and during the other half period, upper right and lower left ones are on. Thus, the RF voltage is connected to the upper winding of the IF transformer with opposite polarity in every LO half period.

In Figure 12, operation is similar to the diode ring mixer, except that the FET switches are controlled by their GS voltages.

3. Analysis Results

The mixers have been analyzed in AWR [17]. RF input is 4 MHz, two tones with a difference of 1 kHz. LO frequency is 5 MHz. IF is investigated around 9 MHz. In the analysis options, 4 harmonics are allowed for all three excitation frequencies. The explanation of why the harmonic number is so low is found in Section 5.3. Legacy harmonic balance solver has been used with absolute and relative error of 10^{-15} and 10^{-5}, respectively.

The following models have been used. As a diode model in Figure 1(b), we included the exponential ideal diode in parallel with a nonlinear junction and diffusion capacitances, all in series with a parasitic resistance and an inductance. Model parameters are $I_0 = 2.918 * 10^{-9}$ A, Nu = 1.9058, $R_s = 0.352$ ohms, $L_s = 10$ nH, $C_0 = 1.57$ pF, and $\tau = 2$ ns. As a jFET model, we use the built-in Spice model with a 300-ohm series gate resistance as shown in Figure 8(b); VP = −6.11 V, IDSS = 693.5 mA, beta = 0.1135, lambda = 0.1597, and CGS = CGD = 18 pF, and as a BJT model, we use the built-in Gummel-Poon model; $\beta = 505$. BJT model accuracy is not critical due to the large emitter resistances.

Analysis results have been compared in Table 1. For OIP3, the multiplier is the best one (see please Figure 22) and for conversion loss, the diode ring mixer. Note that, for isolation between LO and IF, the half H with diodes is the weakest.

4. Measurement Results

The mixers have been assembled on prototype breadboards. For semiconductors, 1N4148 type diode, BC109C type BJT, and J108 type jFET have been used. In earlier versions, we also experimented with BF240, J309, J310, J107, and 2N7000. Model parameters have been determined using least square

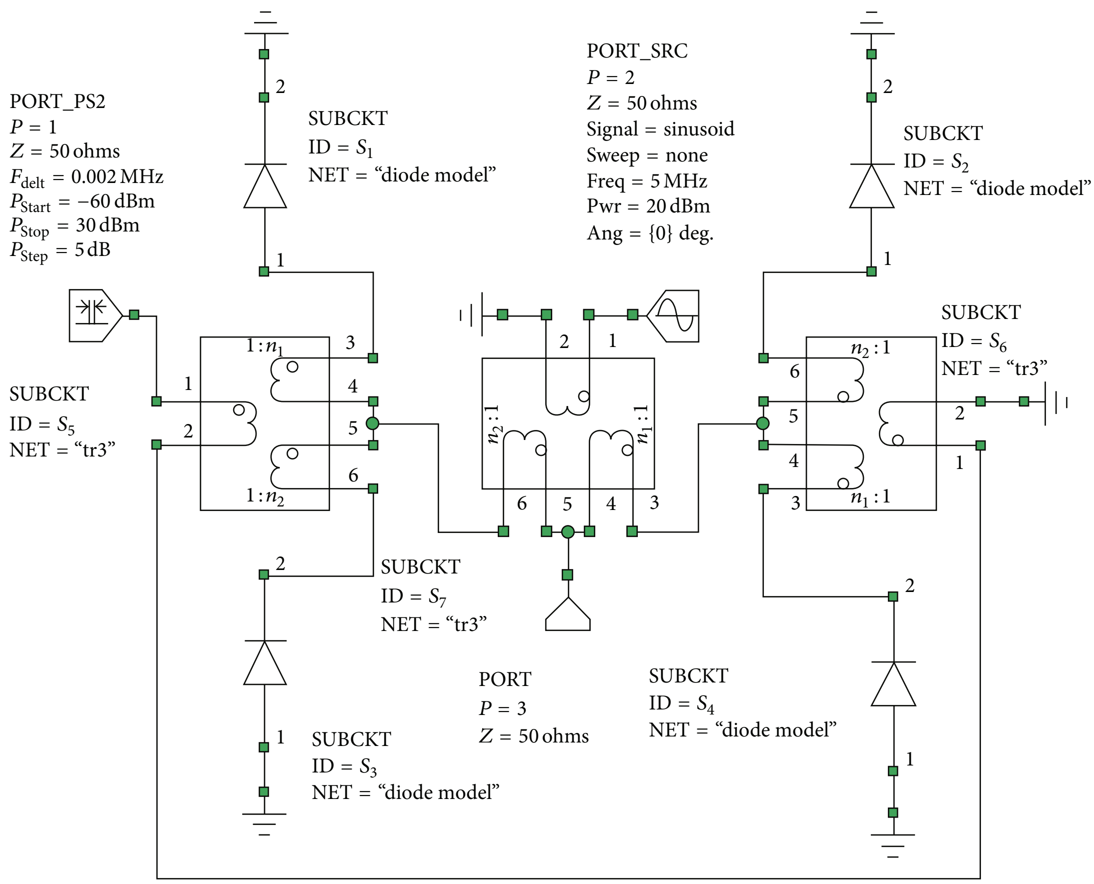

Figure 6: Schematics of the H mixer with diodes.

Table 1: Analysis results.

	Conversion loss at 0 dBm RF	OIP3 at 0 dBm RF	OIP3max at PRF	IIP3max at PRF	PLO at RF port at 0 dBm RF	PLO at IF port at 0 dBm RF
	dB	dBm	dBm	dBm	dBm	dBm
2-diode mixer	11.2	6.73	10.56 at +5	21.76 at +5	−15.8	−28.1
4-diode ring mixer	4.45	12.18	14.18 at −5	18.63 at −5	−23.28	−55.83
8-diode triple balanced	6.74	10.29	14.83 at +10	21.57 at +10	−22.99	−65.62
8-diode rectifier type	5.24	13.84	14.9 at −10	20.14 at 10	−22.27	−32.29
Half H with diodes	7.97	13.49	13.49 at 0	21.46 at 0	−21.38	16.63
Full H with diodes	7.76	12.27	17.53 at +10	25.29 at +10	33.59	−152.3
Four-quadrant multiplier*	5.48		See pls. Figure 22		−294.9	−93.23
Half H	5.4	16	23.8 at +5	29.2 at +5	−58.11	−19.33
Half H, Russian type	6.56	14.1	23.3 at +20	29.86 at +20	−58.79	−19.6
Original full H	4.86	11.84	17.78 at +5	22.64 at +5	−35.5	−49.49
Simplified H	5.4	12.4	24.6 at +10	30 at +10	−58.05	−71.24
FET ring	5.36	12.5	24.6 at +10	29.96 at +10	−55.82	−71.32

*None of them needs DC supply except the four-quadrant multiplier, ±12 V 30 mA.

fitting for DC measurements and by a capacitance meter. Model parameters are shown in the previous section.

Modeling was a crucial part of this work. In order to achieve as small deviation from the measurement results as possible, transformers and semiconductors are needed to be modeled properly. Since IP3 is very sensitive to transformer parameters, this model includes the coupling coefficient and the parasitic capacitances of the coils. For the diode model, I_0, VT, the series resistance, and the junction capacitance at zero bias have been measured. Setting up the JFET model

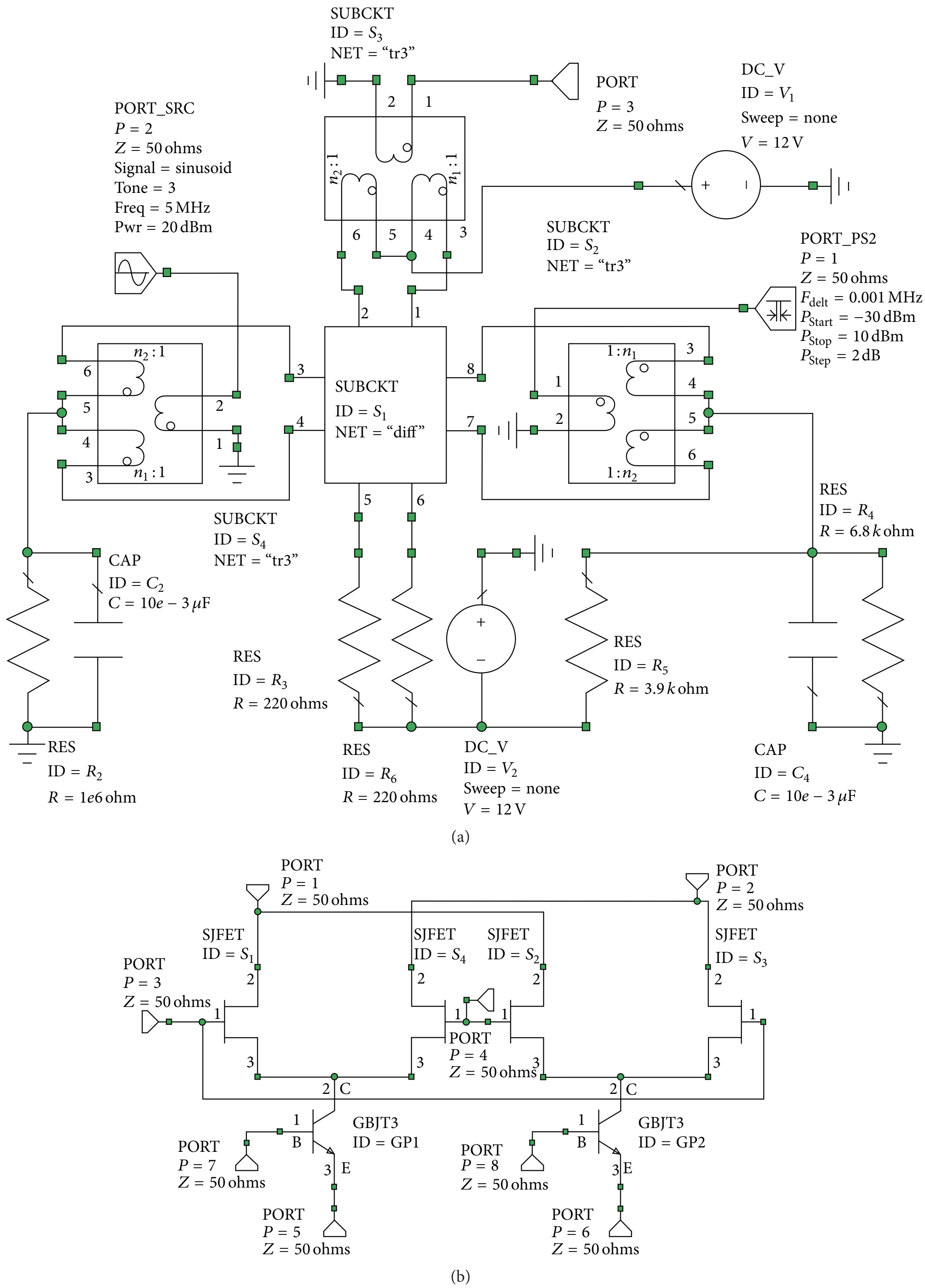

FIGURE 7: (a) Schematics of the four-quadrant multiplier. A small modification: BJT amplifiers operate here in nondifferential configuration. (b) Details of the subcircuit diff for Figure 7(a).

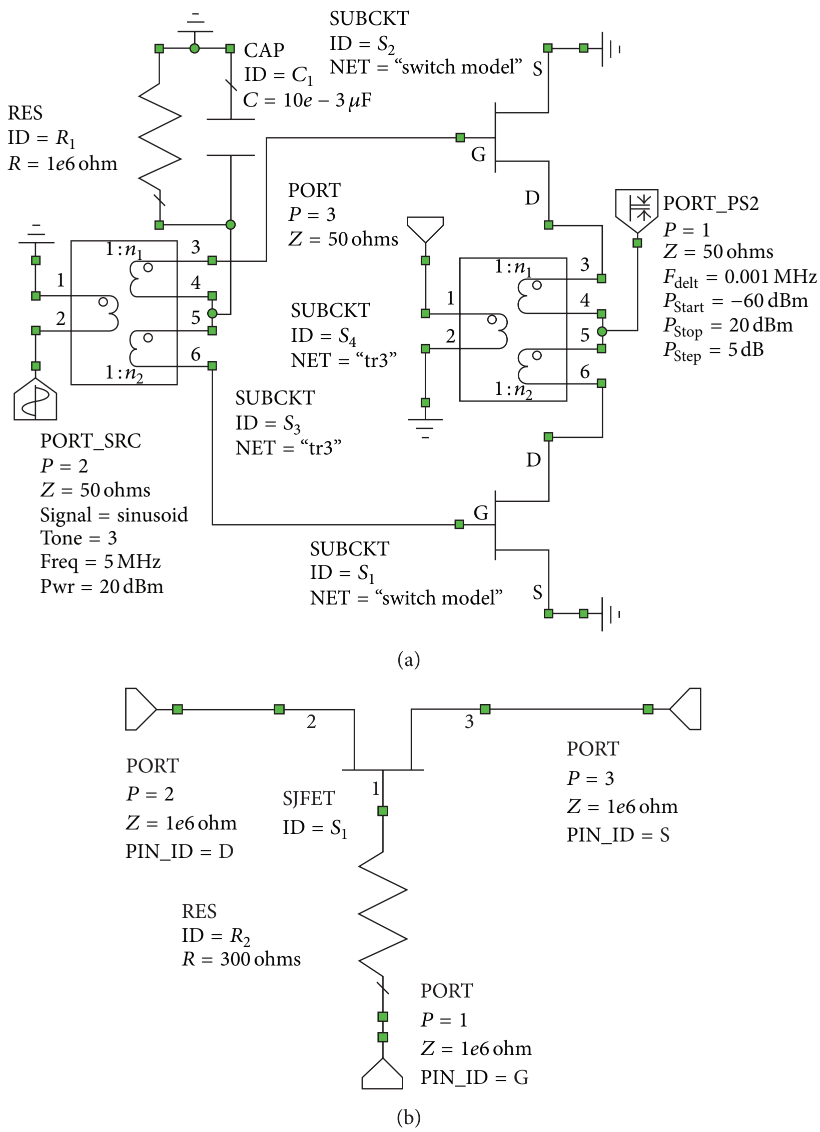

FIGURE 8: (a) Schematics of the half H mixer. (b) Switch model for Figures 8(a), 9, 10, 11, and 12.

requires the measurement of the FET's pinch-off voltage and drain current for zero bias.

We have also made extended measurements using Kundert's method [18]. It is significant that an alternative for IP3 measurement is offered on the basis of the dependence of the IF fundamental tone on the RF input power, but the evaluation is very sensitive to the measurement inaccuracies and the convergence properties of the applied curve fitting method. Moreover, this method does not take into account the nonresistive properties of the mixer; however, with increasing frequency, they become essential.

We used a spectrum analyzer Agilent N9010A, a signal generator Agilent E4433B, and a function generator Agilent 33250A. The applied LO and RF signals are 5 MHz and 4 MHz with the power of +20 dBm and −30 to +10 dBm adjustable, respectively. The IF output has been investigated with the spectrum analyzer around 9 MHz. For the IP3 measurements, two-tone signal has been used with a frequency difference of 1 kHz. OIP3 has been measured at 0 dBm RF input power.

Figure 13 shows the spectrum of the IP3 measurement. The picture was taken during the measurement of the diode ring mixer.

Figure 14 shows the results of first-order product (P1) and third-order intermodulation product (P3) versus RF input power measurements of the two-diode mixer.

It can be seen that the slope of the third-order intermodulation product's curve is not constantly three times greater than that of the first-order product over the investigated RF input power range. The LO to RF and LO to IF isolations were measured at 0 dBm RF input power. The results of these measurements were −44.36 dBm and −37.4 dBm, respectively. Compared to the analyzed results, deviations can be observed. This deviation is present at every other mixer in this paper and it is caused by the transformer and semiconductor asymmetry. From the first-order and

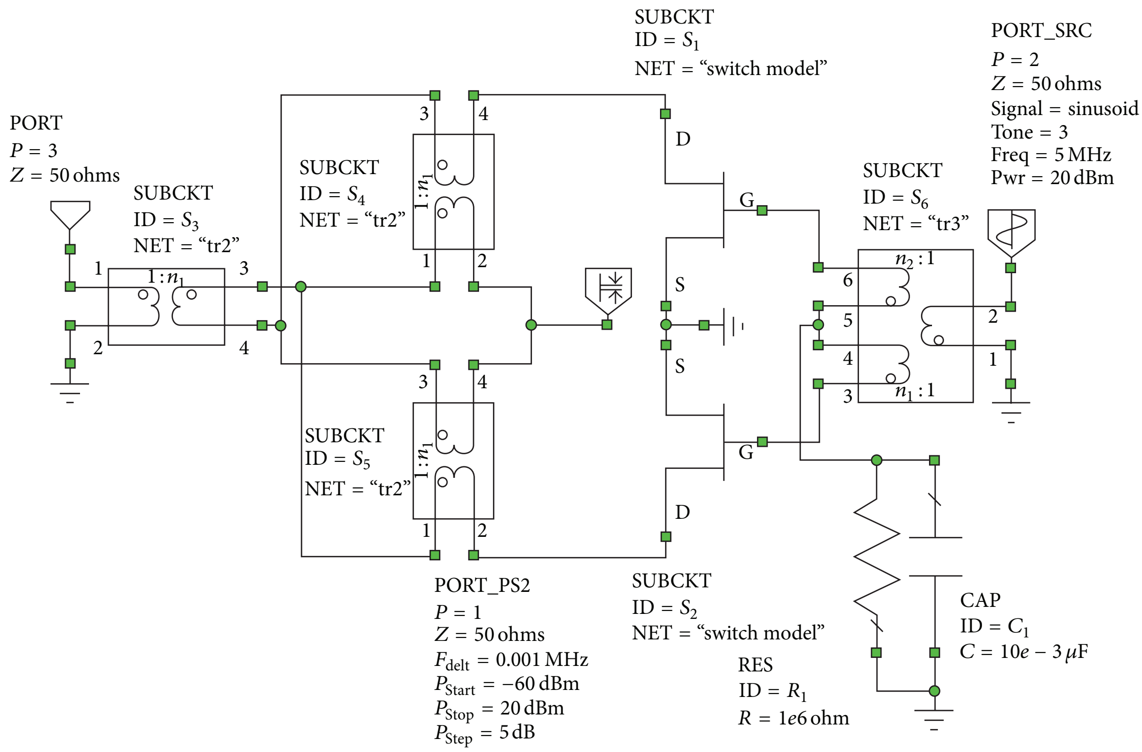

FIGURE 9: Schematics of the Russian type modified half H mixer. Modification with respect to the original version [6] is the replacement of the 4-winding IF transformer by a 2-winding one and interchange of the RF and IF ports; these are our contributions. Also, in [6] it is not clear how the upper and lower two coils of S_4 and S_5 are coupled. As shown in this figure, our interpretation is that they are uncoupled.

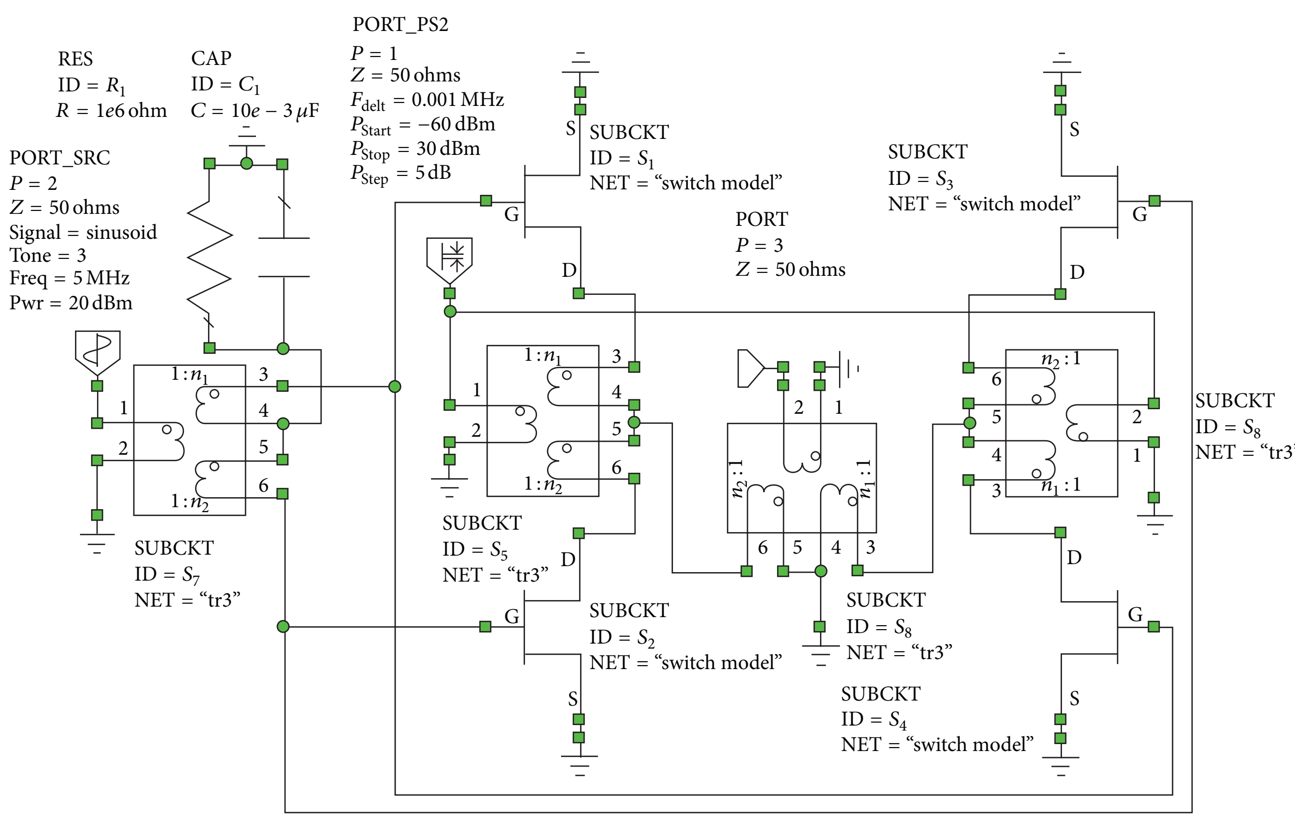

FIGURE 10: Schematics of the original full H mixer.

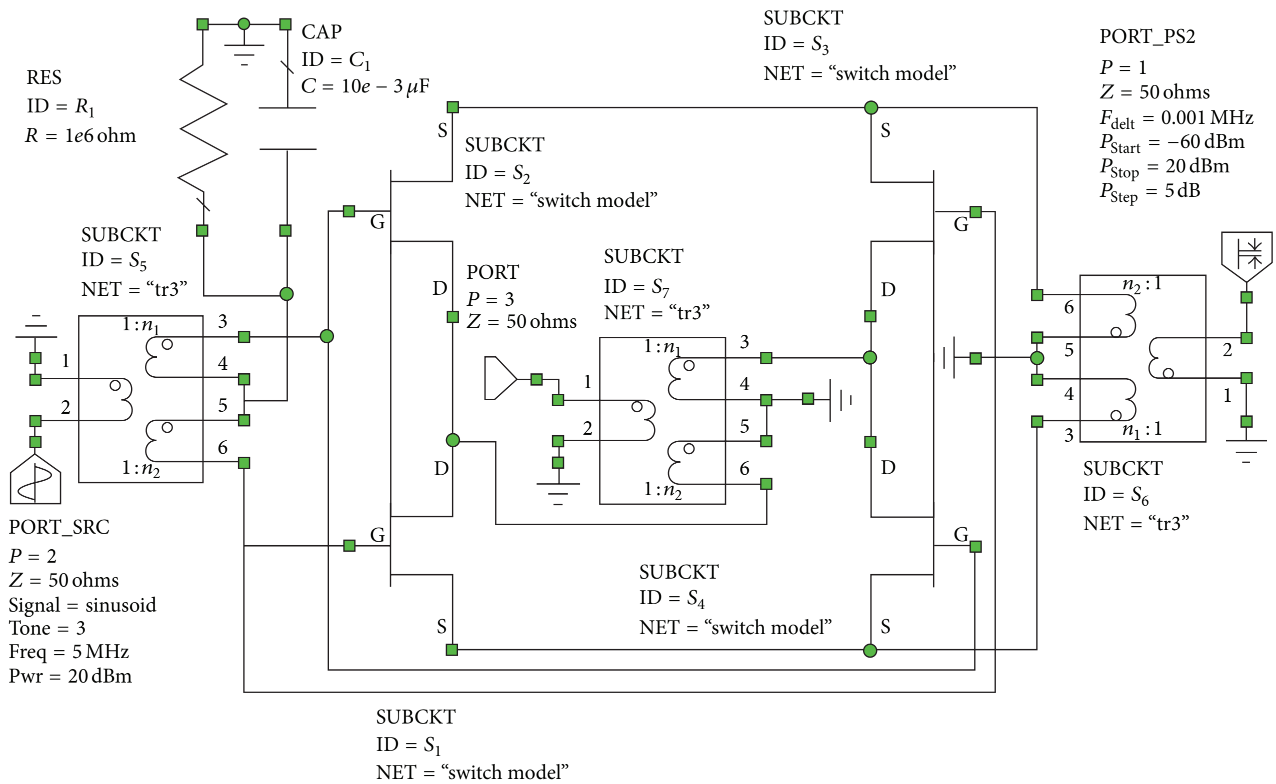

FIGURE 11: Schematics of the simplified H mixer. Simplifications with respect to Figure 10 are the use of fewer transformers and the method of feeding the RF; these are our contributions.

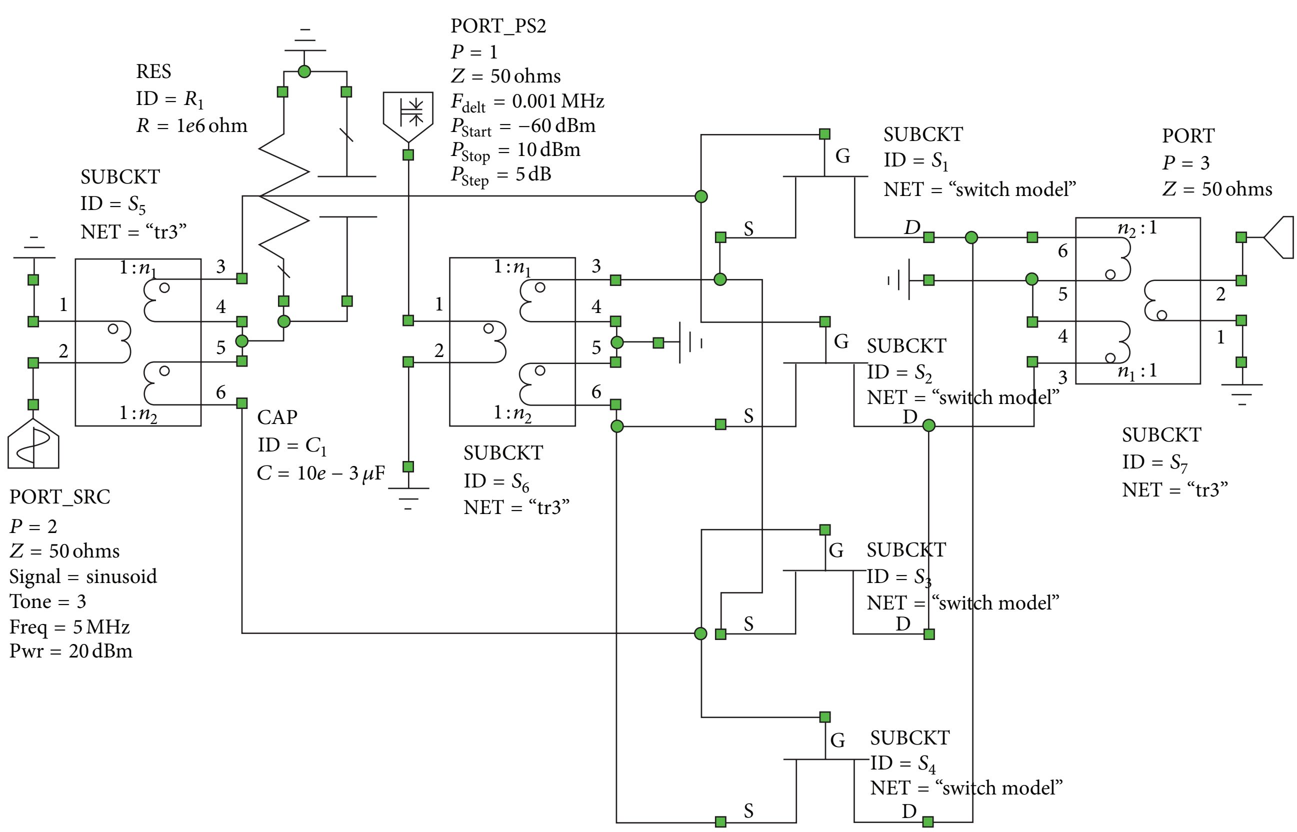

FIGURE 12: Schematics of the FET ring mixer.

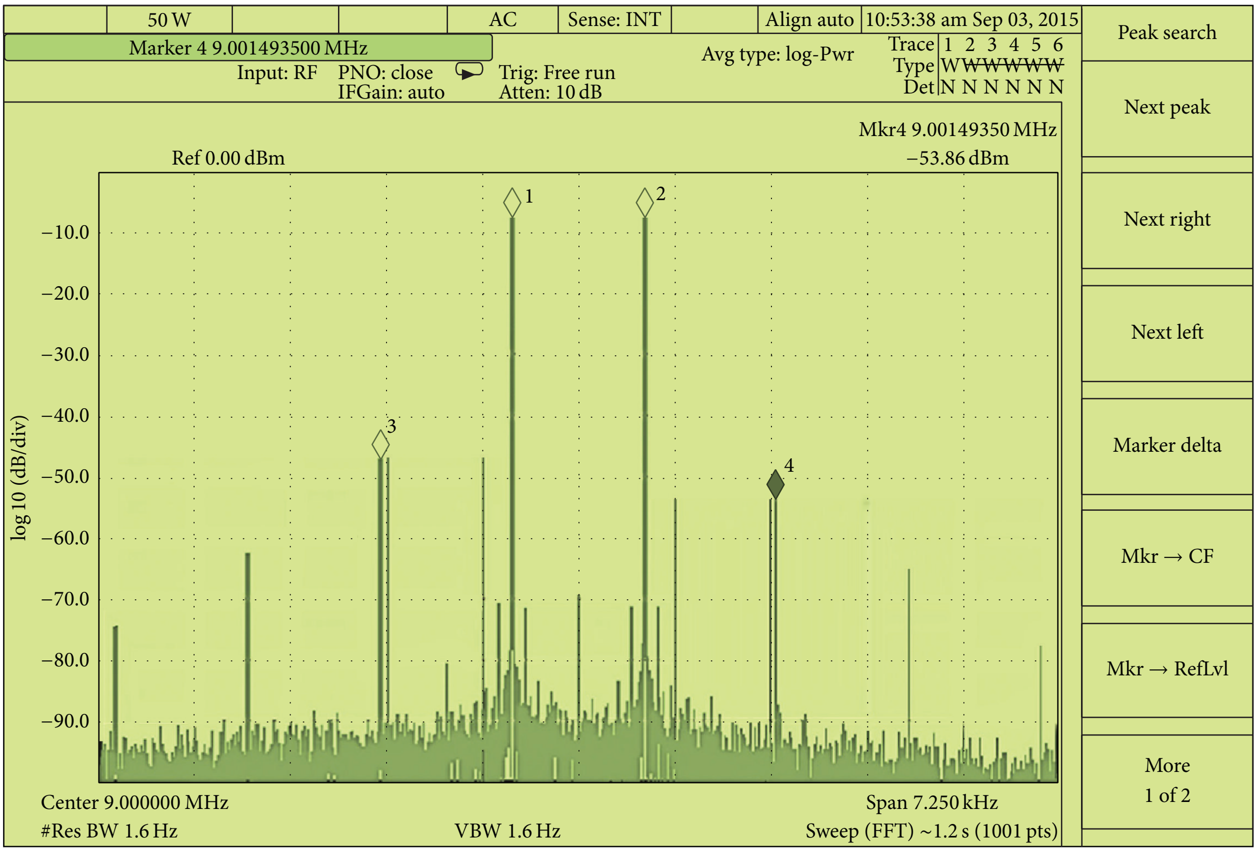

FIGURE 13: Spectrum of the IP3 measurement. The first-order products were 9.0005 MHz and 8.9995 MHz whereas the third-order products were 9.0015 and 8.9985 MHz signals.

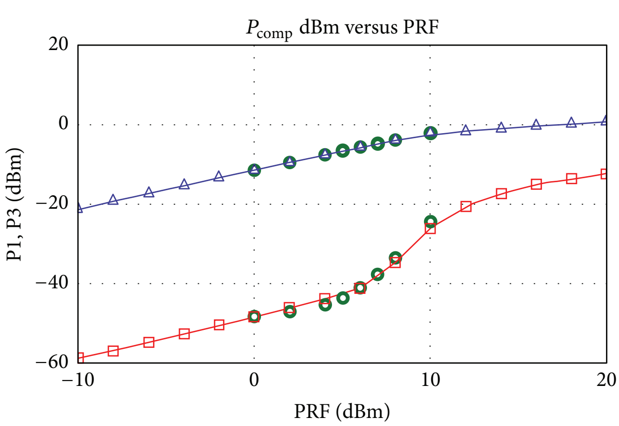

FIGURE 14: First-order product (P1) and third-order intermodulation product (P3) versus RF input power of the two-diode mixer. Blue triangles: analyzed P1; red squares: analyzed P3; green circles: measurement.

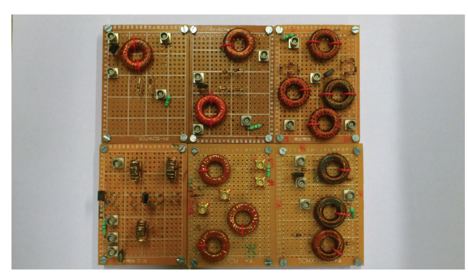

FIGURE 15: Diode mixers. From left to right, upper row: the two-diode mixer, the diode ring mixer, and the triple balanced mixer; lower row: the rectifier type diode mixer, the diode half H mixer, and the diode H mixer.

third-order product powers at 0 dBm RF input, the OIP3 is measured as 7.02 dBm that agrees well with the analysis result. The two-diode mixer exhibits 11.76 dB conversion loss in close agreement with the analysis.

For all other mixers, measurements similar to Figure 14 were made.

Figure 15 shows the diode mixers. In Figure 16 the assembled transistor mixers can be observed.

Agreement between analysis and measurement of conversion loss and OIP3 is very good, while isolations are reproduced in qualitative manner. Table 2 shows that the original full H exhibits the lowest measured conversion loss, whereas the four-quadrant multiplier performs the highest IP3 (infinite, Figure 22). For the measured LO-RF and LO-IF isolation, original full H and the FET ring are the best ones.

Table 2: Comparison of analysis and measurement.

	Conversion loss At 0 dBm RF		OIP3 At 0 dBm RF		PLO at RF port At 0 dBm RF		PLO at IF port At 0 dBm RF	
	Anal dB	Meas dB	Anal dBm	Meas dBm	Anal dBm	Meas dBm	Anal dBm	Meas dBm
2-diode mixer	11.2	11.76	6.73	7.02	−15.8	−44.36	−28.1	−37.4
4-diode ring mixer	4.45	7.08	12.18	13.41	−23.28	−24.99	−55.83	−62.36
8-diode triple balanced	6.74	7.007	10.29	10.87	−22.99	−10.16	−65.62	−70.9
8-diode rectifier type	5.24	7.726	13.84	15.29	−22.27	−22.27	−32.29	−48.51
Half H with diodes	7.97	9.02	13.49	11.68	−21.38	−17.02	16.63	18.01
Full H with diodes	7.76	5.93	12.27	11.41	33.59	−29.9	−152.3	−45.54
Four-quadrant multiplier*	5.48	5.59	See pls. Figure 22		−294.9	−51.05	−93.23	−62.14
Half H	5.4	5.02	16	11.89	−58.11	−32.91	−19.33	−29.88
Half H, Russian type	6.56	5.46	14.1	11.59	−58.79	−18.63	−19.6	−31.11
Original full H	4.86	4.09	11.84	12.67	−35.5	−53.95	−49.48	−54.62
Simplified H	5.4	4.73	12.4	11.68	−58.05	−44.37	−71.24	−67.99
FET ring	5.36	4.87	12.5	11.85	−55.82	−46.4	−71.32	−76.65

*None of them needs DC supply except the four-quadrant multiplier, ±12 V 30 mA.

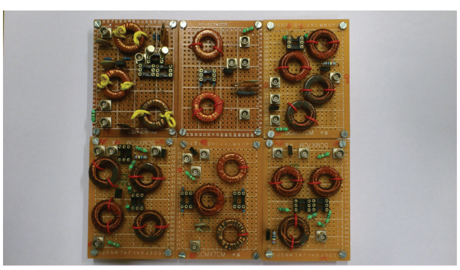

Figure 16: FET mixers. From left to right, upper row: the four-quadrant multiplier, the half H mixer, and the Russian version of the half H mixer; lower row: the full H mixer, the simplified full H mixer, and the FET ring mixer. jFETs and BJTs are inserted into 2 × 3 IC sockets.

5. Improvement of Large Signal Performance

5.1. Diplexer at RF Port. Use of a diplexer [11] with a mixer is well known, but at the IF port. Mixer is preceded by a preamplifier or a filter (Figure 17) that can show exotic termination for the mixer at high frequencies. As good harmonic termination of the mixer input is important, we suggest here a diplexer (Figure 18) between the filter and the mixer RF port. In common terminology, diplexer is a three-port device that separates frequency bands of transmission from the input to the two output ports. However, the device in Figure 18 is also commonly called diplexer. The diplexer cannot substitute the filter, because frequency characteristics are much less demanding than those of a good filter. In our case, the diplexer connects the RF input of the mixer to the filter output with low loss in the passband and terminates both the mixer and the filter by 50 ohms in the stopband. Next we compare OIP3 of a filter-mixer combination with and without a diplexer between them (Figure 19).

It is shown in Figure 19 that the inclusion of a diplexer results in 5–8 dB improvement in OIP3. Here, a diode ring mixer has been applied but similar result can be obtained using other type of mixers as well.

5.2. Reduction of DC Currents. This method means reduction of DC currents alone while AC currents remain intact. We present this method applying to the rectifier type mixer. In Figures 20(a) and 20(b), a rectifier type mixer without using this method is shown. Reduction of DC currents is shown in Figures 21(a) and 21(b). Improvement in OIP3 is about 7 dBm.

5.3. Exploiting a Region of Infinite IP3. In the recent literature, competition for achieving high IP3 was tight. But one can ask if there is an upper limit of IP3 or it can be infinite.

In the recent literature, competition for achieving high IP3 was tight. But one can ask if there is an upper limit of IP3 or it can be infinite.

We have to distinguish interpolated and real IP3. Interpolated IP3 is the power level (input: IIP3, output: OIP3) where the lines that fit to the first- and third-order intermodulation power level versus input power curves intersect each other. Real IP3 is where intermodulation curves intersect each other. Obviously, real IP3 cannot be infinite, but we show that interpolated IP3 can.

At lower RF power, first- and third-order intermodulation products as functions of RF input approximate straight lines. Slope of the third-order product line is expected as three times greater than that of the other line. But Figure 22 shows that this is not the case; the two curves can be parallel and that means infinite IP3. In Figure 22, this region is between −20 and +2 dBm RF power.

In Figure 22 it is obvious that if a region of infinite IP3 exists, then real IP3 occurs at a higher level than without it.

But the main importance of infinite IP3 region is a warning: if we specify IP3, then the corresponding RF power range should always be mentioned.

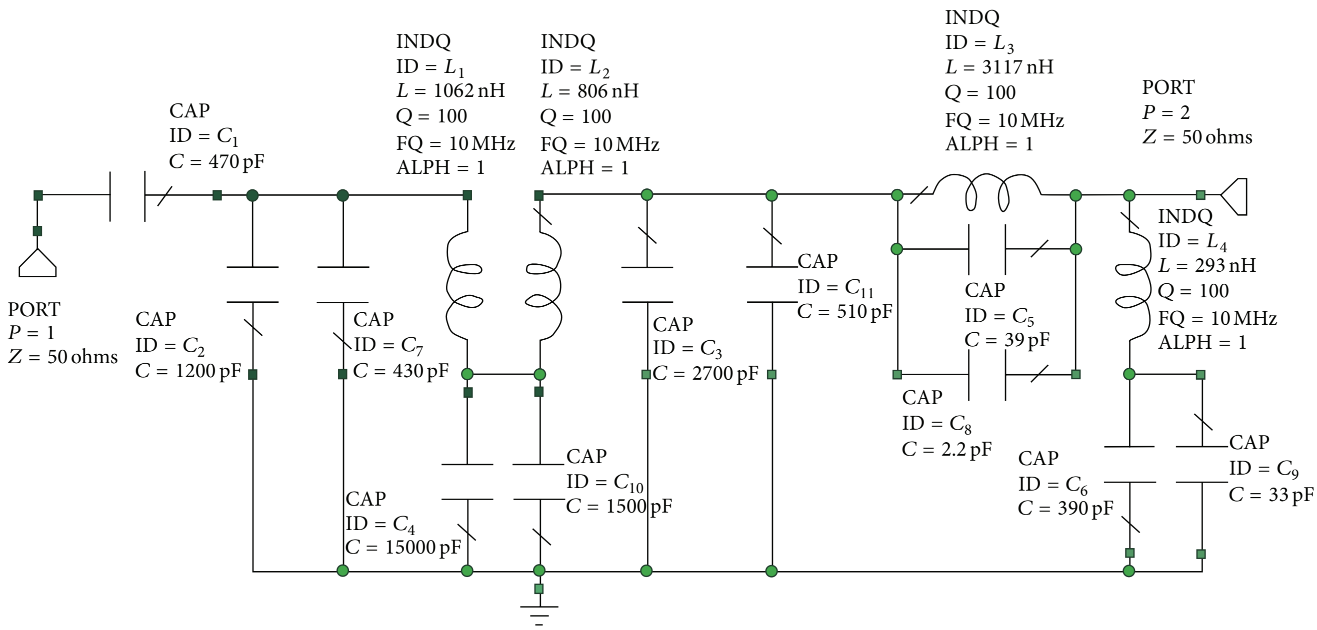

FIGURE 17: RF filter.

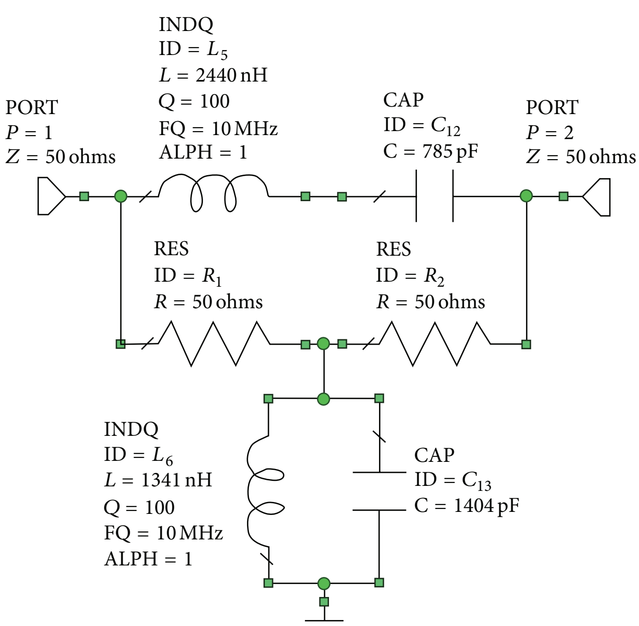

FIGURE 18: Diplexer [11]. The two bands are the neighborhood of the passband and outside. In the passband, low loss transfer is realized; outside of the passband both ports are terminated by 50 ohms, while transfer between ports is attenuated.

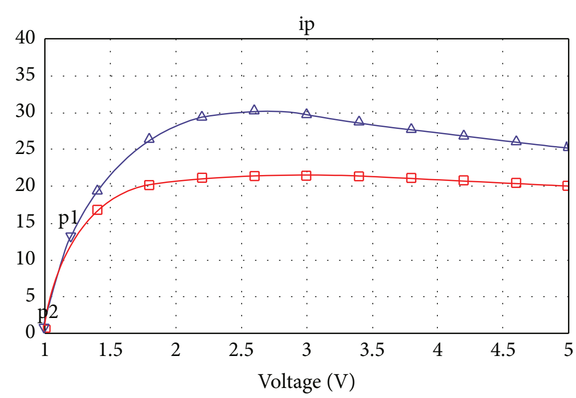

FIGURE 19: Simulated OIP3 in dBm versus LO amplitude level in volts without (red squares) and with (blue triangles) diplexer at RF port of the diode ring mixer. LO signal is a square wave; RF inputs are two tones of −20 dBm, with 2 kHz frequency difference.

The question is what causes infinite IP3. The material of the applied toroidal ring Amidon T68-2 is responsible for that. Cutoff frequency is about 30 MHz; thus IF harmonics above the fourth one are deeply attenuated. If we apply more than four harmonics in the analysis, then infinite IP3 disappears immediately.

6. Conclusion

In this paper we presented a complete picture about semiconductor mixers with good large signal properties. As far as IP3 at 0 dBm RF is considered, our modification of the four-quadrant multiplier (Figure 7(a)) is the best one. But we note that several other criteria may occur such as simplicity (2-diode mixer), properties above 0 dBm RF (original full H) or isolation between ports (diode ring).

We compared large signal analysis results and measurements of large signal properties of twelve different mixers. Simulation and measurement results are in a good agreement. Conditions of comparison were the same LO level and identical transformer inductances.

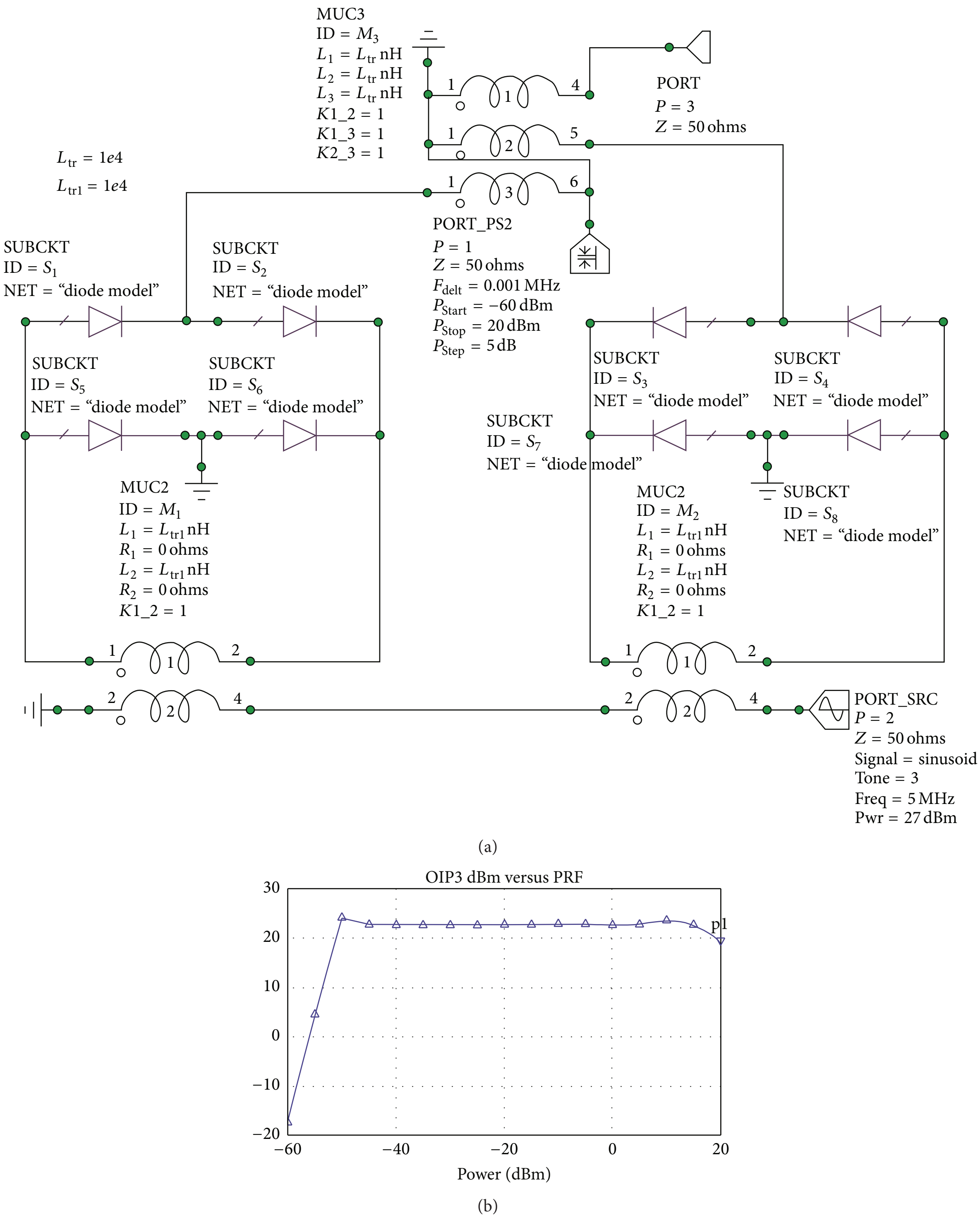

Figure 20: (a) Rectifier type mixer, no DC current reduction. LO of +27 dBm. (b) OIP3 versus RF input power for the rectifier type mixer without DC current reduction.

Our goal was not to achieve record highest possible for IP3. In order to do that, we can use higher LO power, higher transformer inductances (high AL) and coupling between coils, higher cutoff frequency of cores, and application of our suggestions to improve large signal performance in Section 5. Instead, besides overview, our secondary goal was to reproduce well the measured conversion loss and OIP3 values in analysis.

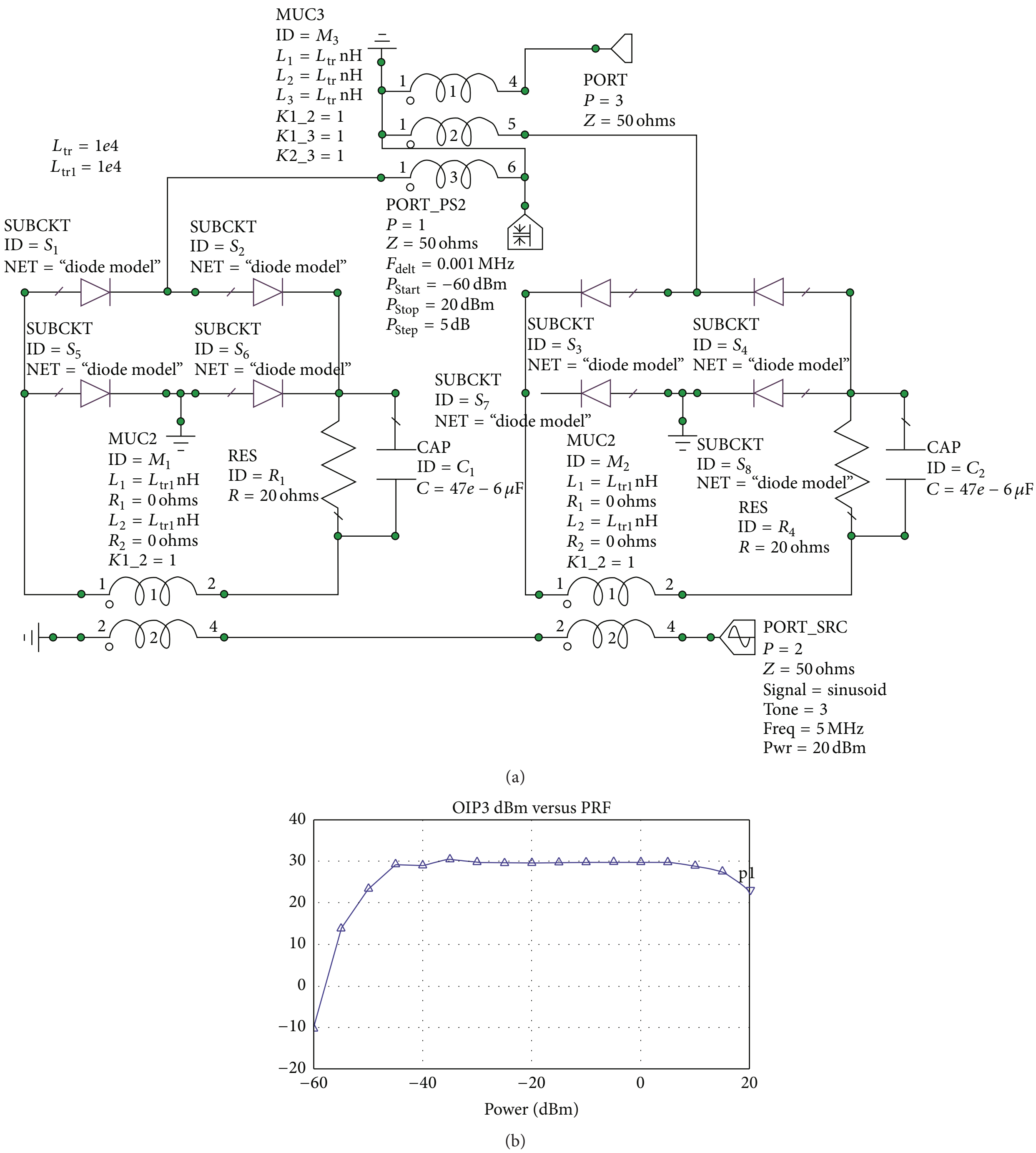

Figure 21: (a) Rectifier type mixer with DC current reduction. LO of +27 dBm. OIP3 is better by 7 dB than with no DC current reduction. (b) OIP3 versus RF input power for the rectifier type mixer with DC current reduction.

We did several modifications to existing mixer configurations as well. The half H mixer with diodes (Figure 5) is completely our contribution. Our plan is to select one mixer from this study and realize it at microwaves. The best candidate is the half H mixer with diodes. Preliminary analysis results at microwaves are encouraging: 8.6 dB conversion loss and 12.5 dB OIP3 at 10 GHz RF of 0 dBm.

In References, our intention was to obtain original ones; however, a foundation work [1] and some most recent mixer papers [15, 16] are also included.

Competing Interests

The authors declare that there are no competing interests regarding the publication of this paper.

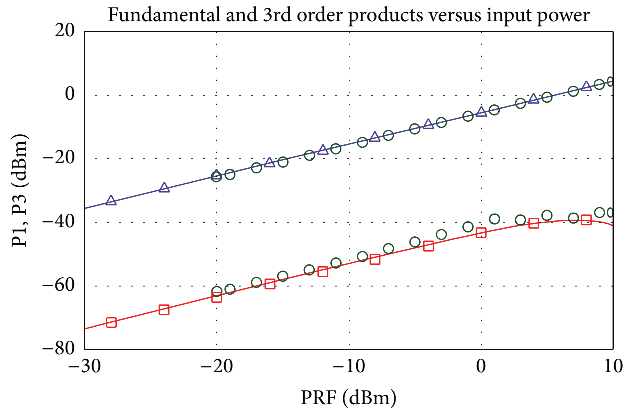

Figure 22: Simulation of the first- and third-order intermodulation products as a function of RF input power of a four-quadrant multiplier in Figures 7(a) and 7(b). Triangles: first-order product; squares: third-order product; circles: measurements.

Acknowledgments

This work has been done at the Ericsson Telecom Hungary (ETH) and a laboratory of the Budapest University of Technology and Economics (BUTE). Thus Mr. Vilmos Beskid and Mr. Ábel Vámos at ETH and Professor Tibor Berceli at the BUTE are greatly acknowledged for providing excellent research conditions. The authors are also grateful to Mr. Boris Dortschy (Ericsson Research, Stockholm, Sweden) and Mr. Tamás Cseh (Budapest University of Technology and Economics, Budapest, Hungary) for the internal reviews. The first author is grateful for Professor Martti Valtonen of the Helsinki University of Technology and Professor Vittorio Rizzoli of the Bologna University of Technology for accepting him as a guest researcher in 1993 and 1994, respectively, and providing him the best algorithms possible for harmonic balance.

References

[1] M. Uhle, "Chua, L. O., C. A. Desoer, E. S. Kuh: linear and nonlinear circuits. McGraw-Hill Book Company, New York 1987, XVII, 839 S., DM 122,40. ISBN 0-07-010898-6," *Biometrical Journal*, vol. 30, no. 7, pp. 867–868, 1988.

[2] W. D. Hope, "Balanced mixer," US Patent, US 2754416 A, July 1956.

[3] P. M. Thompson, "Diode ring circuit," US Patent, US 2923894 A, February 1960.

[4] B. C. Henderson, "Mixers, Part 2: Theory and Technology," Watkins Johnson Communications.

[5] *Year-Book of Radio Technics (in Hungarian)*, Rádióvilág Ltd, Budapest, Hungary, 2015.

[6] C. Trask, *Mixer Musings and the KISS Mixer*, 2012, http://www.mikrocontroller.net/attachment/146369/Mixer_Musings.pdf.

[7] H. E. Jones, "Dual output synchronous detector utilizing transistorized differential amplifiers," US Patent, US 3241078 A, March 1966.

[8] D. Gamliel, "Double balanced FET mixer with high IP3 and IF response down to DC levels," US Patent, US 6957055 B2, February 2002.

[9] E. S. Oxner, "Commutation mixer achieves high dynamic range," *RF Design*, pp. 47–53, 1986.

[10] R. Setty and D. Ji, "Triple Balanced Mixer," US Patent, US 6917796 B2, September 2002.

[11] https://en.wikipedia.org/wiki/Diplexer.

[12] V. Rizzoli, C. Cecchetti, A. Lipparini, and F. Mastri, "General-purpose harmonic balance analysis of nonlinear microwave circuits under multitone excitation," *IEEE Transactions on Microwave Theory and Techniques*, vol. 36, no. 12, pp. 1650–1660, 1988.

[13] Keysight Technologies, "IMD Measurement with E5072A ENA Series Network Analyzer," http://www.keysight.com/upload/cmc_upload/All/ENA_IMD_Measurement_Summary.pdf.

[14] J. Ladvánszky, "Circuit theoretical aspects of optical communication links," in *Proceedings of the 17th International Conference on Transparent Optical Networks (ICTON '15)*, Budapest, Hungary, July 2015.

[15] J. Zhang, M. Bao, D. Kuylenstierna, S. Lai, and H. Zirath, "Transformer-based broadband high-linearity HBT Gm-boosted transconductance mixers," *IEEE Transactions on Microwave Theory and Techniques*, vol. 62, no. 1, pp. 92–99, 2014.

[16] N. M. Amin, Z. G. Wang, and Z. Q. Li, "Folded down-conversion mixer for a 60 GHz receiver architecture in 65 nm CMOS technology," *Journal of Zhejiang University SCIENCE C*, vol. 15, no. 12, pp. 1190–1199, 2014.

[17] NI AWR Design Environment, http://www.awrcorp.com/.

[18] K. Kundert, *Accurate and Rapid Measurement of IP2 and IP3*, Version 1b, The Designer's Guide Community, 2002.

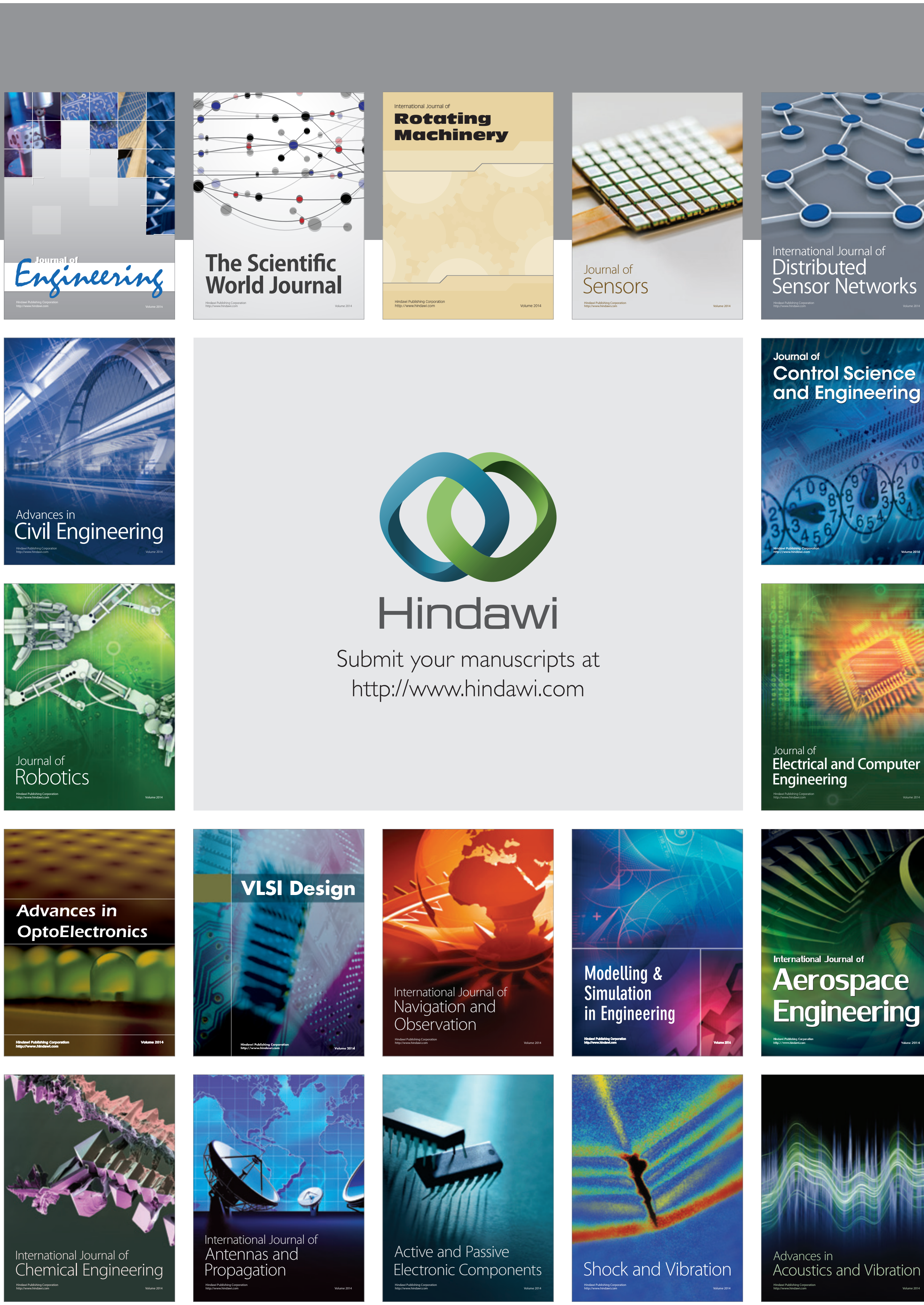

Journal of Engineering
The Scientific World Journal
International Journal of Rotating Machinery
Journal of Sensors
International Journal of Distributed Sensor Networks
Advances in Civil Engineering
Hindawi
Submit your manuscripts at
http://www.hindawi.com
Journal of Control Science and Engineering
Journal of Robotics
Journal of Electrical and Computer Engineering
Advances in OptoElectronics
VLSI Design
International Journal of Navigation and Observation
Modelling & Simulation in Engineering
International Journal of Aerospace Engineering
International Journal of Chemical Engineering
International Journal of Antennas and Propagation
Active and Passive Electronic Components
Shock and Vibration
Advances in Acoustics and Vibration